

Terahertz surface plasmon resonance microscopy based on ghost imaging with pseudo-thermal speckle light

Ildus Sh. Khasanov¹, Lydia A. Zykova¹, Alexey K. Nikitin¹, Boris A. Knyazev^{2,3}, Vasily V. Gerasimov^{2,3} and Ta Thu Trang⁴

¹Scientific and Technological Center for Unique Instrumentation of RAS, Moscow 117342, Russia

²Budker Institute of Nuclear Physics SB RAS, Novosibirsk 630090, Russia

³Novosibirsk State University, Novosibirsk 630090, Russia

⁴Russian-Vietnamese Tropical Center, Hanoi, Vietnam

Abstract— Surface plasmon resonance (SPR) microscopy is one of the most sensitive optical label-free methods of metal/semiconductor surface microscopy. Nevertheless, it does not have sufficiently high lateral resolution. This is due to the fact that surface plasmon polaritons excited by terahertz (THz) radiation propagate from their excitation spot over macro distances (about $\sim 100 \lambda$), thereby blurring the observed area, by analogy with a scattering medium. To eliminate this disadvantage, we propose to adapt the single-pixel imaging technique known as ghost imaging (GI), which is notable for its tolerance to environmental aberrations between an object and a camera. To implement the classical GI for THz SPR microscopy we propose to use spatially modulate light by speckle patterns arising from the reflection of coherent THz radiation (generated by a free electron laser) from a rough metal surface.

I. INTRODUCTION

SPR microscopy is widely used [1] due to the simplicity of the method. Terahertz (THz) plasmonics has numerous applications in non-destructive testing of thin films [2,3] by virtue of its ultra-high vertical resolution of objects with sizes up to $\lambda/100$. However, as was noted by many researchers, including the inventor [4], the main disadvantage of SPR microscopy is its low lateral resolution.

The lateral resolution of a SPR microscopy is influenced by many factors, but the most important physical reason is that the area of localization of surface plasmon polaritons (SPPs) excited by a light beam exceeds the spot on the surface. So SPPs propagate along the interface from the excitation spot and are randomly reradiated into the prism (see Fig. 1), which introduces spurious illumination. This additional illumination “blurs” the resulting image of the surface. The distance over which the SPPs propagate is determined by the losses due to their scattering on the roughness of the metal and absorption in it and the covering layer. For THz SPPs on metal the average distance L_x , at which the SPPs field intensity decreases by a factor of e , can be sufficiently large (about $\sim 100 \lambda$) [5].

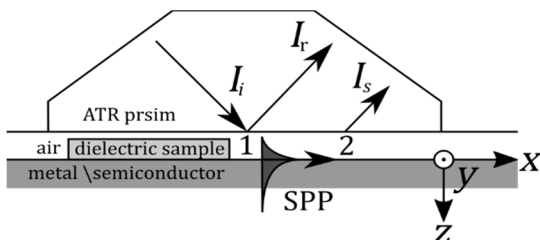


Fig. 1. A schematic diagram explaining the mechanism of SPP reradiation outside the excitation point. I_i — incident radiation, I_r — reflected radiation, I_s — scattered radiation from SPP.

II. RESULTS

The image of the object $O(x, y)$ in ghost imaging (GI) is restored by calculating the second-order correlation function between the spatial distribution of the probe beam light intensity $P(x, y)$ (patterns) and the integrated intensity S of the reflected (or transmitted) light from an object received by a single-pixel detector in two optical paths (x, y) and (x', y') :

$$O(x, y) \propto \langle P(x, y)_i \cdot S_i \rangle - \langle P(x, y) \rangle \langle S \rangle, \quad (1)$$

where $\langle \dots \rangle = \frac{1}{N} \sum_{i=1}^N \dots$ — is the averaging operator, N is the number of independent patterns, $R(x', y')$ is the object response function.

To create different patterns $P(x, y)$ in the computational GI, the light field is structured using a special device such a spatial light modulator (SLM), and thus the probing beam is known a priori, which allows one to avoid using a camera. Nevertheless, for now, in THz range, GI were not able to achieve high-resolution images due to the lack of high-resolution SLMs. However, in classical optical nanoscopy [6] GI renders possible to obtain high-resolution images using speckle patterns. In the THz range speckle patterns easy to implement and their properties are well known [7]. THz speckles can be observed with a microbolometer array using a high power free electron laser (FEL).

We can highlight two important advantages of GI. First, GI is lensless: we don't need any lens to register a probe beam on the camera. Thus, we avoid and aberrations and significant energy losses in optics. This is important because THz cameras are optics-limited in contrast with diffraction-limited visible range cameras. Secondly, in GI an object is observed by the detector with no spatial resolution. Thus, GI is tolerant to

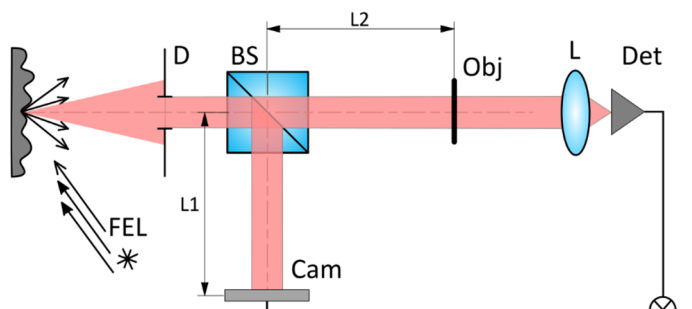


Fig. 2. Scheme of classical ghost imaging: FEL — laser source; D — diaphragm; BS — non-polarizing beam splitter; Obj — object; Det — single-pixel detector; L — collecting lens; Cam — multi-pixel camera; L1 — distance between camera and beamsplitter; L2 — distance between detector and beamsplitter. In the best-case scenario $L1=L2$.

aberrations in the optical path between the object and the single-pixel detector. This property initially was used to neglect image blurring caused by light scattering in a turbulent medium. Taking this advantage, we propose to adapt GI to the traditional SPR microscopy scheme to eliminate spurious illumination from re-emitted SPPs. For this purpose, we use an ATR prism in place of the object in the classical GI scheme (see Fig. 2). Referring to Figure 1, we can decompose detected radiation into two components:

$S_i = \int R(x', y')(P(x', y')_i + I_s(x', y')_i) dx' dy' = So_i + Sc_i$, where $P(x', y') = P(x, y)$ is light intensity distribution on the surface of a thin film (or an object under study), So_i is the object signal, Sc_i is the spurious signal. Obviously, the spurious illumination from SPPs excited at the spot (x_1, y_1) and randomly reradiated at other point on the surface (x_2, y_2) does not depend on the intensity of radiation incident on (x_2, y_2) , that means:

$$\langle P(x, y)_i \cdot I_s(x', y')_i \rangle = \langle P(x, y) \rangle \langle I_s(x', y') \rangle.$$

Then the image in the ghost SPR microscopy can be found as:

$$\begin{aligned} O(x, y) &\propto \langle P(x, y)_i \cdot (So_i + Sc_i) \rangle - \langle P(x, y)_i \rangle \langle So_i + Sc_i \rangle \\ &= \langle P(x, y)_i \cdot So_i \rangle - \langle P(x, y) \rangle \langle So \rangle = O_o(x, y). \end{aligned}$$

Thus, we have shown that GI eliminates the effect of blurring from re-emission of SPPs, and we obtain the unbiased image $O_o(x, y)$ of the investigated surface.

To analyze the factors affecting the resolution of proposed method, we can represent the estimated image $O_o(x, y)$ of the investigated surface as the sum of two parts:

$$O_o(x, y) = \iint R(x', y') C_s(x - x', y - y') dx' dy' + \langle P(x, y) \rangle^2 \iint R(x', y') dx' dy', \quad (2)$$

where the correlation function C_s :

$$C_s(x - x', y - y') = \langle P(x, y)P(x', y') \rangle - \langle P(x, y) \rangle \langle P(x', y') \rangle$$

The first term in sum (2) is responsible for lateral resolution, and the second term in sum (2) affects the vertical resolution of the surface in SPR microscopy (contrast of ghost image). And the noise in the estimated image can be reduced by increasing the number of measurements (with collection of independent speckle patterns). So with an increase in the number N of measurements signal-to-noise (SNR) improves as $\text{SNR}(N) \propto \sqrt{N} \text{ SNR}(1)$.

We can identify the following main factors affecting the resolution: 1) the lateral resolution is affected by speckle size and the misalignments of wavefronts between the camera and the object plane; 2) the vertical resolution is affected by the sensitivity of the receivers, stability of the source, background illumination and spurious illumination from SPPs.

Let us present schematically a GI simulation algorithm for reconstructing images of a semiconductor surface coupled with an ATR prism under illumination with speckle structures (see Fig. 3). We simulate the light distribution corresponding to the speckle patterns $P(x, y)$ using the Fourier transform (FT) of the field of random spatial frequencies $p(k_x, k_y) = FT[P(x, y)]$. To take into account the diffraction properties of the diverging beam, we obtain the angular spectrum of the speckle pattern using the inverse Fourier transform (IFT) and then correct it using the known resonance curve $R(\theta)$ for each spatial frequency $R^d(x', y') = IFT[p(k_x, k_y)R(\theta)]O(x, y)$. We repeat this procedure for each area of the surface $R(x', y') = \sum R^d(x', y')$, taking into account the corresponding resonance

curve — the form of this curve depends on the optical properties of the dielectric coating and its thickness d , and in the case of the Otto configuration, on the size of the gap between the prism and semiconductor as well (see Fig. 1).

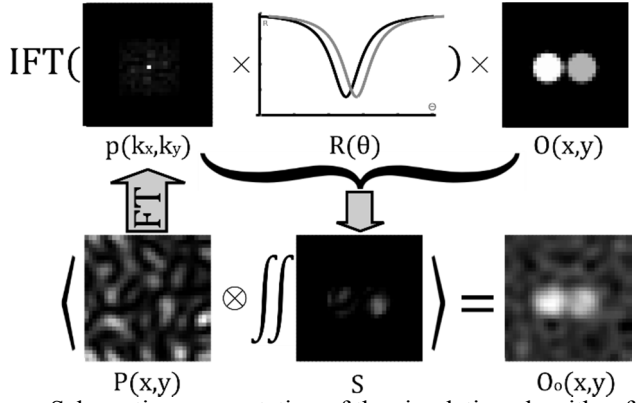


Fig. 3. Schematic representation of the simulation algorithm for image obtained by GI SPR microscopy. In simulation, image resolution is 32x32 pixels and total number of speckle patterns $N = 1000$.

III. SUMMARY

From our analysis it follows that the GI adapted to SPR microscopy can significantly improve the lateral resolution capability by eliminating the effect of a SPP reradiation. On the basis of simulation, we assume that classical ghost imaging can be easily implemented in practice for terahertz SPR microscopy with pseudo-thermal speckle light produced by coherent THz radiation sources such as FEL. The work was supported by the Russian Foundation for Basic Research (project 20-52-54004) jointly with VAST (project QTRU01.03/20-21).

REFERENCES

- [1]. X.-L. Zhou, Y. Yang, S. Wang, and X.-W. Liu, "Surface Plasmon Resonance Microscopy: From Single-Molecule Sensing to Single-Cell Imaging," *Angewandte Chemie International Edition*, vol. 59, no. 5, pp. 1776–1785, 2020, doi: [10.1002/anie.201908806](https://doi.org/10.1002/anie.201908806).
- [2]. A.K. Nikitin, O.V. Khitrov, V.V. Gerasimov, I.S. Khasanov, and T.A. Ryzhova, "In-plane interferometry of terahertz surface plasmon polaritons," *J. Phys.: Conf. Ser.* 1421, 012013, 2019, doi: [10.1088/1742-6596/1421/1/012013](https://doi.org/10.1088/1742-6596/1421/1/012013).
- [3]. I. Sh. Khasanov, V. V. Gerasimov, and A. K. Nikitin, "Spectral radiation pattern of bulk waves emitted by thermally stimulated surface plasmons at the sample edge," in 2019 44th International Conference on Infrared, Millimeter, and Terahertz Waves (IRMMW-THz), Paris, France, Sep. 2019, pp. 1–2, doi: [10.1109/IRMMW-THz.2019.8874496](https://doi.org/10.1109/IRMMW-THz.2019.8874496).
- [4]. E. Yeatman and E. A. Ash, "Surface plasmon microscopy," *Electronics Letters*, vol. 23, no. 20, p. 1091, 1987, doi: [10.1049/el:19870762](https://doi.org/10.1049/el:19870762).
- [5]. V. V. Gerasimov, B. A. Knyazev, A. G. Lemzyakov, A. K. Nikitin, and G. N. Zhizhin, "Growth of terahertz surface plasmon propagation length due to thin-layer dielectric coating," *Journal of the Optical Society of America B*, vol. 33, no. 11, pp. 2196–2203, 2016, doi: [10.1364/JOSAB.33.002196](https://doi.org/10.1364/JOSAB.33.002196).
- [6]. W. Li *et al.*, "Single-frame wide-field nanoscopy based on ghost imaging via sparsity constraints," *Optica*, vol. 6, no. 12, pp. 1515–1523, 2019, doi: [10.1364/OPTICA.6.001515](https://doi.org/10.1364/OPTICA.6.001515).
- [7]. N.A. Vinokurov, M.A. Dem'yanenko, D.G. Esaev, B.A. Knyazev, G.N. Kulipanov, O.I. Chashchina, and V.S. Cherkasskii, "Speckle pattern of the images of objects exposed to monochromatic coherent terahertz radiation," *Quantum Electron.*, vol. 39, no. 5, pp. 481–486, 2009, doi: [10.1070/QE2009v03n05ABEH013950](https://doi.org/10.1070/QE2009v03n05ABEH013950).